SIMULATIONS OF THE INTERACTIONS OF SILICON WITH CARBON NANOTUBES

by

Michael P. Fogarty

A senior thesis submitted to the faculty of

Brigham Young University

in partial fulfillment of the requirements for the degree of

Bachelor of Science

Department of Physics and Astronomy

Brigham Young University

April 2009

BRIGHAM YOUNG UNIVERSITY

DEPARTMENT APPROVAL

of a senior thesis submitted by

Michael P. Fogarty

This thesis has been reviewed by the research advisor, research coordinator, and department chair and has been found to be satisfactory.

Date	Bret Hess, Advisor
Date	Eric Hintz, Research Coordinator
Date	Ross L. Spencer, Chair

ABSTRACT

Simulations of the Interactions of Silicon with Carbon Nanotubes

Michael P. Fogarty

Department of Physics and Astronomy

Bachelor of Science

This study examines the interaction of silicon with carbon nanotubes(CNTs) as well as graphene. In this process the diffusion properties of silicon on CNTs and graphene were modeled. Using the computer program Fireball the behaviors of these systems were studied. The diffusion barriers for silicon and carbon on the surface of graphene were shown to be 0.42 eV and 0.93 eV respectively at zero temperature. The diffusion barrier for silicon on a graphene sheet at higher temperatures is shown to be 0.36 eV. The model of diffusion of a silicon atom on a graphene sheet is shown for temperatures in the range of 500 K to 3500 K. Various rolled hexagonal-planar formations of silicon nanotubes were shown to be stable with and without a carbon nanotube inside them.

Acknowledgements

I would like to acknowledge and thank my advisor Dr. Bret Hess for guiding me through this research and writing process. I would like to thank my research group for their input and work. They are Daniel Jensen, Peter Lyon, Reid Kraniski, and Scott Horton. I would like to thank my family for supporting me though all of this work especially my parents Mike and Gina. I would like to thank my uncle Danny Fogarty for his advice and editing. Lastly, I want to acknowledge BYU for giving me the opportunity to work on this research.

Table of Contents

List of Figures

Chapter 1: Introduction

1.1 Importance of Carbon Nanotubes

Carbon nanotubes were discovered in 1991 by Sumio Iijima and they consist of a graphene sheet rolled into a seamless tube with capped ends (see Figure 1). Single walled nanotubes (SWNTs) range from about 2-10 nanometers in diameter and can be as long as a few centimeters. SWNTs have exhibited amazing mechanical and electrical properties. They are ideal for applications in reinforced composite materials and nanoelectro-mechanical systems (NEMS): Young's modulus is over 1 TPa and the tensile strength is an estimated 200 GPa. Additionally, SWNTs have very interesting band structures and the electronic properties can be metallic or semiconducting in nature, making it possible to create nanoelectronic devices, circuits, and computers using SWNTs [6].

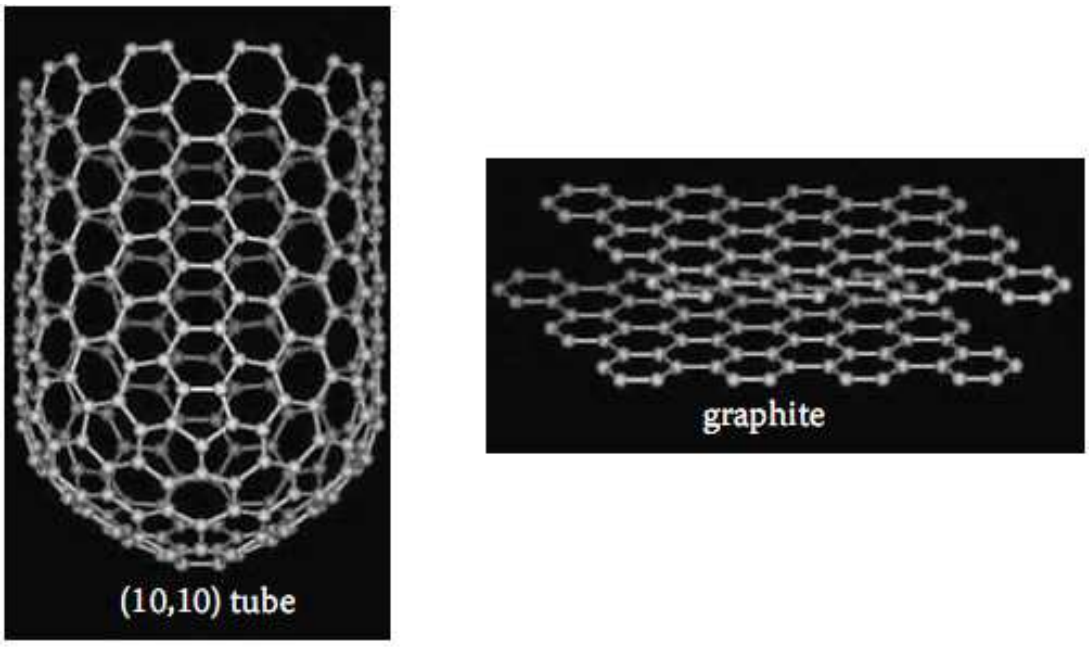

Figure 1- C(10,10) SWNT and Graphene Sheet

1.2 Silicon Nanotubes and Rings

Silicon is widely recognized as the most important material of the 20th century due to its role as the fundamental component in integrated circuits and in the microelectronic revolution [10]. Carbon nanotubes have been subject to extensive research both theoretical and experimental. It is important to study their silicon counterparts. Nanoscale forms of silicon have been investigated by many both for the purpose of further miniaturizing the current microelectronic devices and the hope of unveiling new properties that often arise at the nanoscale. Until recently the studies involving SiNTs have been purely theoretical and although some SiNTs have been grown experimentally none of the models provide a realistic way to grow these structures or study their special characteristics [10]. Results from theoretical data obtained from density functional theory on three SiNTs: the (6,6), which has an armchair structure, the (10,0), which has a zigzag structure, and the (8,2), which has a mixed structure, showed that the electronic properties of single walled silicon nanotubes are very similar to the equivalent of carbon nanotubes. Studies using a full potential linear muffin tin orbital molecular dynamics have simulated stable forms of SiNTs shown below.

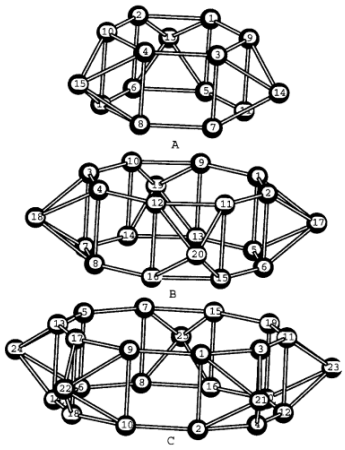

Figure 2- Stable ring structures of Si_{15}, Si_{20}, and Si_{25} [3].

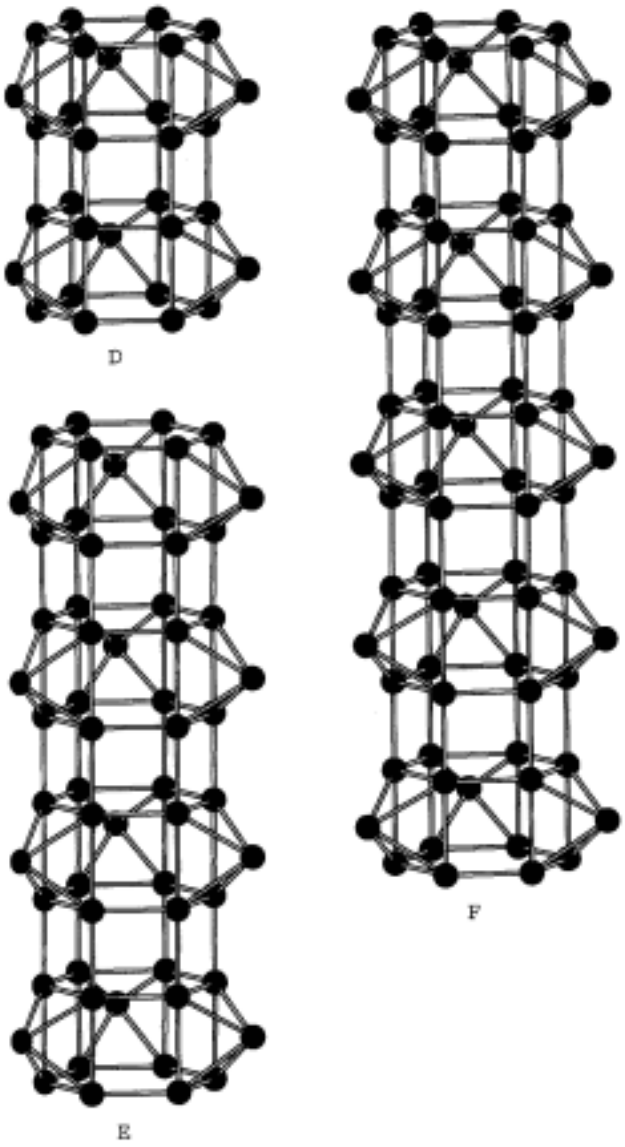

Figure 3- The rings are then stacked to form the stable tube structures. Stable tube structures of Si_{30}, Si_{60}, and Si_{75} [3].

The experimental synthesis of such nanotubes has been demonstrated by various groups. The various models for growth of these nanostructures have not been very consistent with the theoretical predictions due to the differing structures that silicon forms in contrast to carbon. Silicon prefers tetrahedral bonding where as carbon is planar and these differences are evident in the theoretical studies above.

1.3 Graphene

As stated before, CNTs are most generally described as sheets of graphene rolled into a seamless tube and capped at the ends. Studying diffusion on the surface of a graphene sheet is a logical step towards eventually studying the diffusion of adatoms on the surface and interior of CNTs. Based on early experiments on defect migration in graphite, it was argued that the carbon interstitial forms no bonds with the atoms in the lattice, and it can easily migrate in the hollow regions between graphene layers with an activation energy of 0.1 eV [2]. Theoretical calculations, on the other hand, predicted a migration barrier of around 0.42 eV [2, 7, 8].

The paper I found to be most similar to my work with graphite is titled Magnetic properties and diffusion of carbon adatoms on a graphene sheet by Lehtinen et al [7]. In this paper they used ab initio methods to study the diffusion of adatoms on the surface of a graphene sheet. They focused on the spin theory's effect on the energy barrier which my work does not concern since the spin effects account for less than 10% of the energy barrier. They studied the energy barrier along the path shown below in Figure 4.

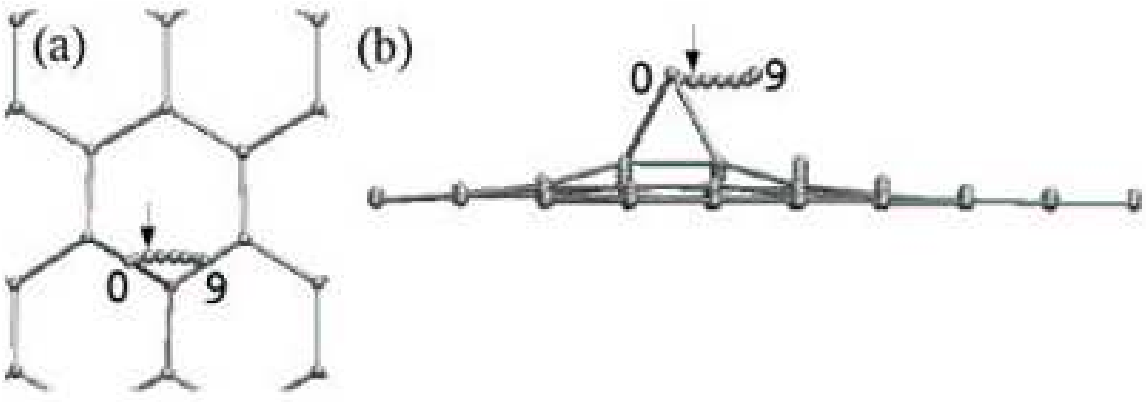

Figure 4- The adatom equilibrium bridge-like position (0) and the diffusion path (0-9) from the (a) top and the (b) side [7].

The calculations were performed using the plane wave basis VASP code, implementing the spin-polarized Density Functional Theory and the GGA of Perdew and the Wang known as PW91. The adatom diffusion path is an almost straight line between the two sites although the minimum energy path was observed to be slightly shifted into the interstitial space in the surface and also slightly nearer the surface than the equilibrium site. The energy barrier was calculated along the path of the adatom and is shown below in Figure 5.

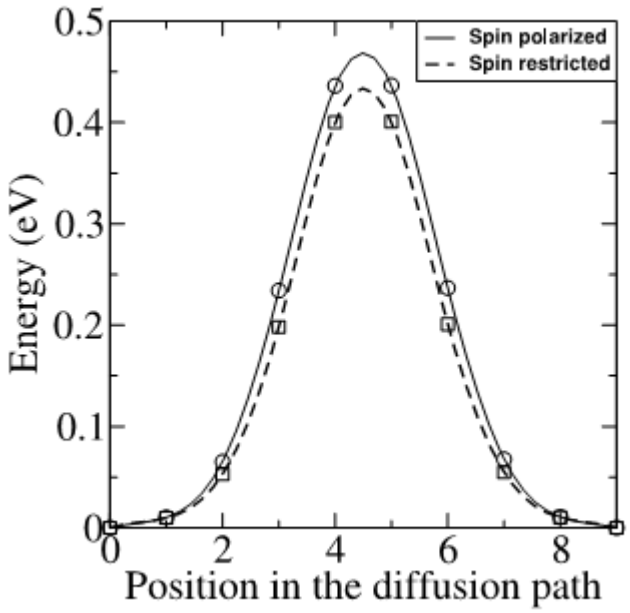

Figure 5- Calculated energy barrier for diffusion of the adatom in the spin polarized and spin restricted case (S=0). The data points are fitted with a cubic spline [7].

The main purpose of this study was to see the effects of magnetic polarization and spin and how it would affect diffusion on the surface of graphite. It was concluded that the effects of the magnetic nature of these adatoms were not huge – changes of only tenths of an eV between the two cases. This is thought to contribute to the magnetism that seems intrinsic to many pure carbon systems. It was concluded that the high mobility of adatoms means that at a high temperature they would be more or less

immediately annihilated by recombination and the magnetic influence would be removed. Also it was concluded that the adatom diffuses as a non-magnetic species and only became magnetic at the equilibrium position [7].

1.4 Bonding on CNTs

My research has been largely based on and motivated by a paper by Durgun et al [4] entitled Energetics and electronic structures of individual atoms adsorbed on carbon nanotubes. In this study extensive investigation was done on the bonding of different types of atoms on the surface of a CNT. The adsorption of individual atoms on the semiconducting and metallic single-walled carbon nanotubes has been investigated using the first principles pseudo potential plane wave method within density functional theory [4]. Figure 6 shows the different sites that the atoms were bonded to and then Figure 7 shows a table of respective energies for many different atoms. This chart was used as reference throughout my research.

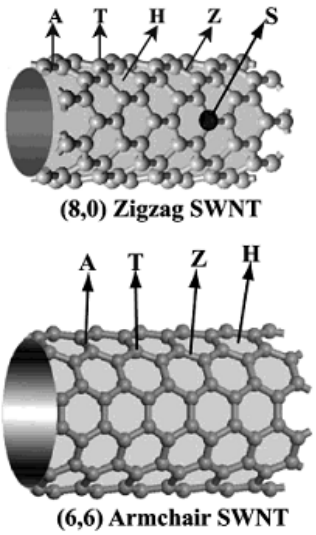

Figure 6- Schematic description of different binding sites of individual atoms adsorbed on both types of SWNTs. H: hollow; A: axial; Z: zigzag; T: top; S: substitution [4].

atom	H(eV)	A(eV)	Z(eV)	T(eV)	ΔE_T(eV)	$\bar{d}_{C-A}$(Å)	$\mu(\mu_B)$
Na	1.3	1.1	1.1	1.1		2.3	
Mg	0.08	0.07	0.05	0.07		3.8–	
Sc	2.1(1.9)	1.4	1.5	→ H	0.15	2.3(2.2)	0.64(1)
Ti	2.9(2.2)	2.1	2.7	2.1	0.58	2.2(2.2)	2.21(4)
V	3.2(1.4)	2.2	→ H	→ H	1.20	2.1(2.2)	3.67(5)
Cr	3.7(0.4)	2.5	→ H	→ H	2.25	2.0(2.3)	5.17(6)
Mn	3.4(0.4)	2.5	→ H	→ H	2.42	2.1(2.4)	5.49(5)
Fe	3.0(0.8)	2.5	→ H	1.6	1.14	2.1(2.3)	2.27(4)
Co	2.8(1.7)	2.5	→ H	→ H	0.41	2.1(2.0)	1.05(3)
Ni	2.2	2.4(1.7)	2.3	→ A	0.02	1.9(1.9)	0.04(2)
Cu	0.5	0.8(0.7)	0.6	→ A	0.03	2.1(2.1)	0.53(1)
Zn	0.05(0.04)	0.05	0.03	0.04	0	3.7(3.7)	0(0)
Nb	3.9(1.8)	2.7	→ H	→ H	0.40	2.2(2.2)	2.86(5)
Mo	4.6(0.4)	3.0	→ H	→ H	0.32	2.2(2.2)	4(6)
Pd	1.1	1.7(1.7)	1.5	1.5	0	2.1(2.1)	0(0)
Ag	0.1	0.3(0.2)	→ A	→ A	0.03	2.7(2.5)	0.6(1)
Ta	2.8(2.4)	2.4	2.5	→ H	0.73	2.1(2.2)	3.01(3)
W	3.4(0.9)	2.5	2.6	3.3	0.59	2.1(2.1)	2.01(6)
Pt	→ Z	2.7(2.4)	2.4	→ A	0	2.1(2.1)	0(2)
Au	0.3	0.6(0.5)	0.4	0.6	0.04	2.2(2.2)	1.02(1)
Al	1.6	1.4	1.5	→ H		2.3	
C	→ Z	3.7	4.2	→ A		1.5	
Si	2.5	2.2	2.5	2.2		2.1	
Pb	1.3(0.8)	1.0	1.2	→ H	0.01	2.6(2.6)	0(2)
H				2.8		1.1	
O			5.1	-		1.5	
S	→ A	2.8	2.4	→ Z		1.9	

Figure 7- Calculated binding energies and average carbon - adatom bond distances, d_{C-A} of individual atoms adsorbed at H, Z, A, and T sites of the (8,0) SWNT as described in Figure 5 [4].

As shown in the table above Group IV elements such as C and Si can be bound with significant binding energy. The H site seems to be the most favorable bonding site for most of the atoms used in this study. This data is very different from the data of adatoms bonded to a graphene sheet and the considerably higher binding energies found for CNTs is most widely attributed to the curvature effect that strengthens the bonding[4].

There have been many studies published claiming that the curvature of nanotubes creates drastic differences between them and graphene. The reported migration barrier of carbon on graphene is about 0.1 eV whereas they are much higher experimentally in CNTs. The migration barriers for one study were reported in the range of 0.6 – 1 eV for SWNTs with typical diameters of 1 – 1.4 nm, which are in good agreement with the experimental values of about 0.8 eV reported in literature [1]. This also suggests a

dependence of the migration barrier upon the corresponding diameter of the tube in question and the tube diameters mentioned are quite small so it is expected that as the tube diameter gets larger the correspondence to graphene will increase.

There have also been studies on the diffusion of carbon atoms inside CNTs. It has been experimentally observed that the migration barrier of carbon interstitials inside the inner hollow of SWNTs of diameter 1.3 nm is about 0.25 eV. This confirmed the theoretical model that predicted that SWNTs could be used as efficient pipelines for the transport of carbon atoms [9].

Chapter 2: Methods

2.1 Programs and Theory

The primary program I used for this study was Fireball. Following is a description of Fireball from The Fireball Manual [11]. Fireball is a first-principles molecular dynamics code made in a density functional tight-binding approach using a basis set of Sankey-Niklewski pseudo-atomic localized atomic orbitals. By comparison to an ab initio code using Hartree-Fock and post-Hartree-Fock methods, or a DFT Kohn-Sham (KS) based approach, the formalism used here follows three main approximations :

1. A substitution of the total energy functional by a functional that has changes of the electron density from that of a sum of neutral atom densities only to first order. This is realized through the use of the Harris-Foulkes functional, which requires in a first step the determination of the band-independent structure energy via resolution of the KS independent particular equations.

2. An approximation of the atomic orbitals (and therefore of the solutions of the independent particle KS equations) by the creation of slightly excited pseudo-atomic localized orbitals. A cutoff, which is more exactly a boundary condition, is defined for each atomic orbital. At this cutoff the orbital is exactly 0. This decreases the number of interactions through space and creates a sparse Hamiltonian matrix for linear-scaling diagonalization.

3. All single-particle Hamiltonian matrix elements are evaluated before the simulations and stored following the idea of the Slater-Koster.

I used TubGen online version 3.3 which is a Web-Accessible Nanotube Structure Generator to generate the structures I used in my simulations [13]. All of the graphics and animations I have created were made using VMD, a molecular visualization and analysis program [14].

Chapter 3: Simulations & Discussion

3.1 Stability of Hexagonal SiNTs on CNTs

I studied the stability of hexagonal silicon nanotubes surrounding carbon nanotubes. I constructed many nanotubes of different chirality and number of atoms and I tried to match up CNTs with SiNTs that were of similar length and with diameters that were compatible. This meant that the CNT radius needed to be at least an angstrom smaller than that of the SiNT so it could fit inside. I gave Fireball the starting position and then relaxed the nanotubes to a very low temperature and compared the movement that took place. I ran all of the nanotubes together with both the C and Si as well as both of the nanotubes separately. The combinations that were studied included: 2xC(6,0) and Si(6,0), C(6,0) and Si(9,0), C(7,0) and Si(7,0), C(8,0) and Si(10,0), and 3xC(8,0) and 2xSi(10,0).

The first combination I used for a CNT surrounded by Si was a 2xC(6,0) with Si(6,0). The start and end pictures are shown below in the figures.

2xC(6,0) Start and Final Positions

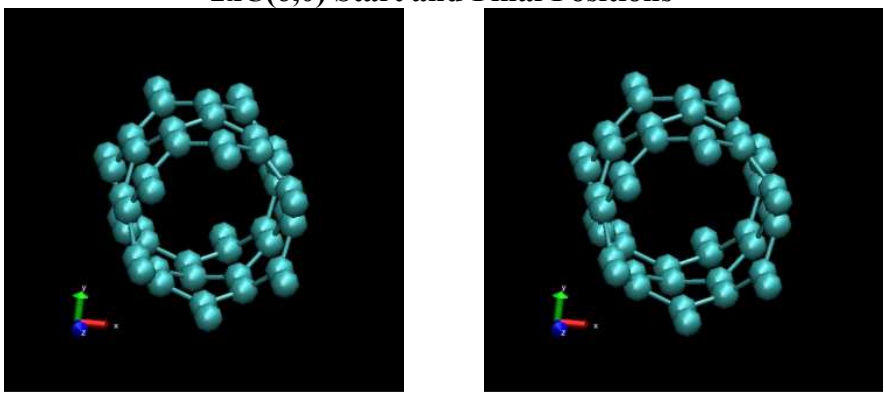

Figure 8- 2xC(6,0) Starting Position and Ending Position. Total Energy per atom was -157.5296 eV and the Final Temperature was 0.1874 K

Si(6,0) Start and Final Positions

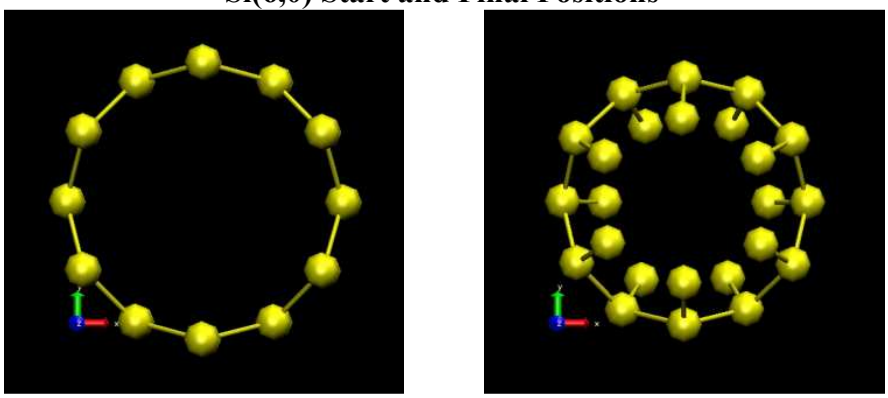

Figure 9- Si(6,0) starting and ending position. Total energy per atom was -107.205514 and the Final Temperature was 27.4679 K

2xC(6,0) and Si(6,0)

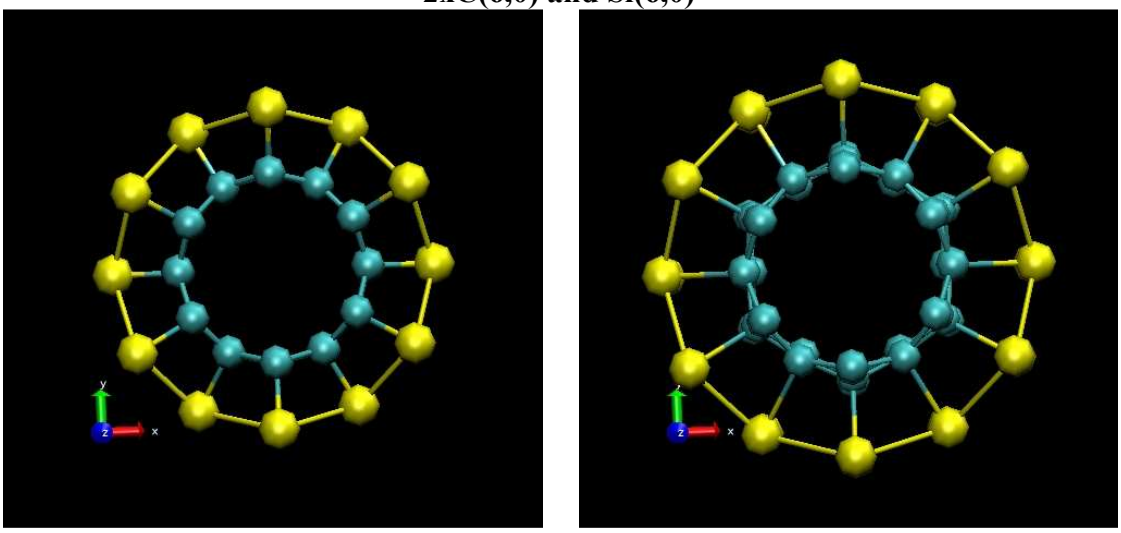

Figure 10- 2xC(6,0) with Si(6,0) starting and ending positions. Total Energy per atom was -140.726 and the Final Temperature was 0.0008 K.

The silicon nanotube seemed much more stable when it was around the CNT as is shown in the figures. They all kept their general shape with the SiNT showing the most distortion.

The next combination I studied was C(6,0) with Si(9,0). The start and final pictures are shown in the figures below with the exception of C(6,0) which is shown above in Figure 10.

Si(9,0) Final Position

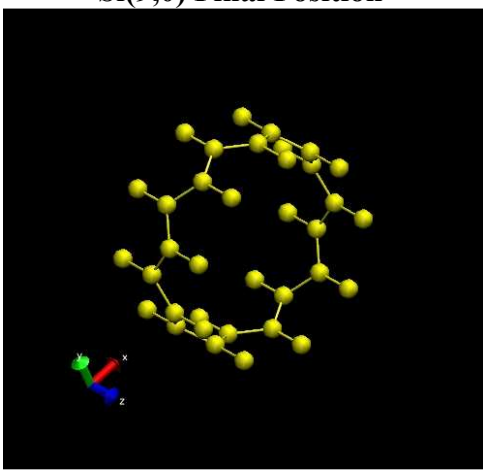

Figure 8- Si(9,0) final position with a temperature of 0.3219 K. Total energy per atom is -107.14658. The tube does not distort hardly at all. It shrinks a little but unlike the Si(6,0) tube the bonds did not bend at all. It also gets to a stable temperature a lot faster than the Si(6,0) tube.

C(6,0) with Si(9,0) Start and Final Positions

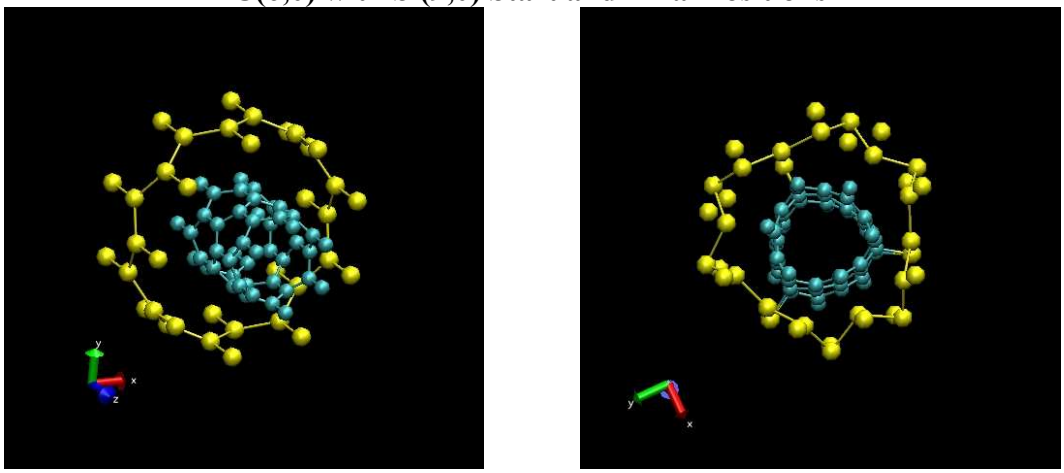

Figure 12- C(6,0) with Si(9,0) starting and ending positions. Final temperature was 1.1126 K and the total energy per atom was -135.93386947 eV. Some of the atoms were unbounded during the relaxation time.

The next combination I did was C(7,0) with Si(7,0) and the final pictures both separate and together are in the figures below.

C(7,0) and Si(7,0) Separate Final Positions

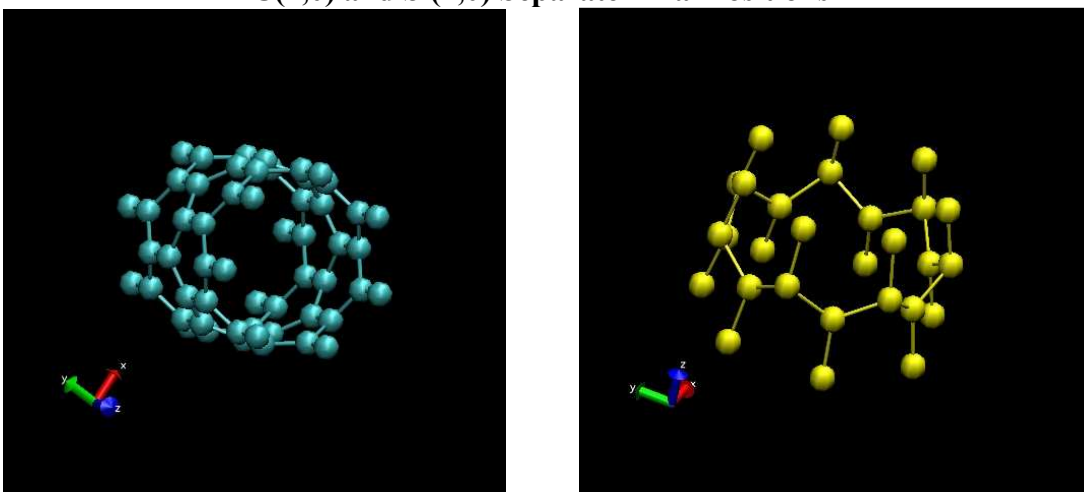

Figure 13- Carbon(blue) and Silicon(yellow) final positions. For carbon the final temperature was 0.0004 K and the energy per atom was -157.619729 eV. For silicon the final temperature was 0.0795 K and the energy per atom was -107.18048 eV.

C(7,0) and Si(7,0) Together Final Position

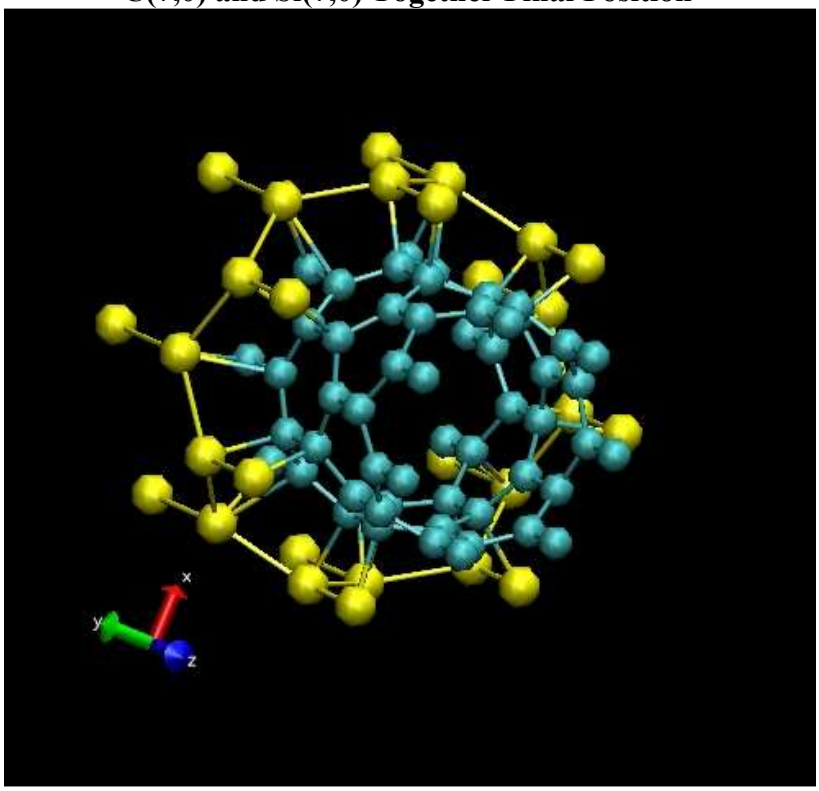

Figure 14- C(7,0) with Si(7,0) final position. The final temperature was 0.0002 K and the energy per atom was -140.76146523 eV. The combined tube behaved as was expected and was very stable when relaxed.

The next combination was C(8,0) with Si(10,0 and the final pictures both separate and together are in the figures below.

C(8,0) Start and Final Positions

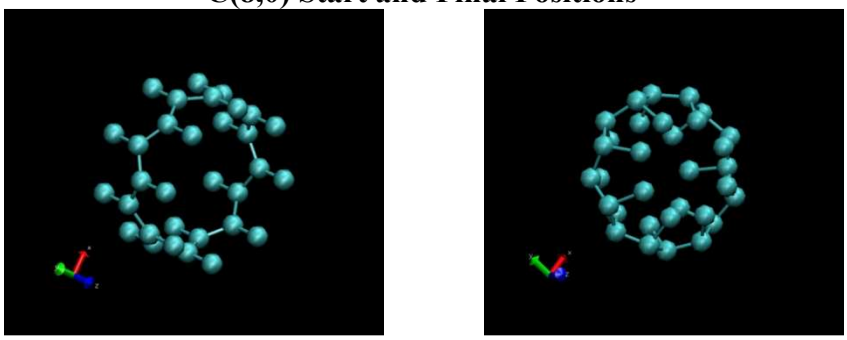

Figure 15- C(8,0) start and final positions. The final temperature was 0.0100 K and the total energy per atom was -156.87817701 eV.

Si(10,0) Start and Final Positions

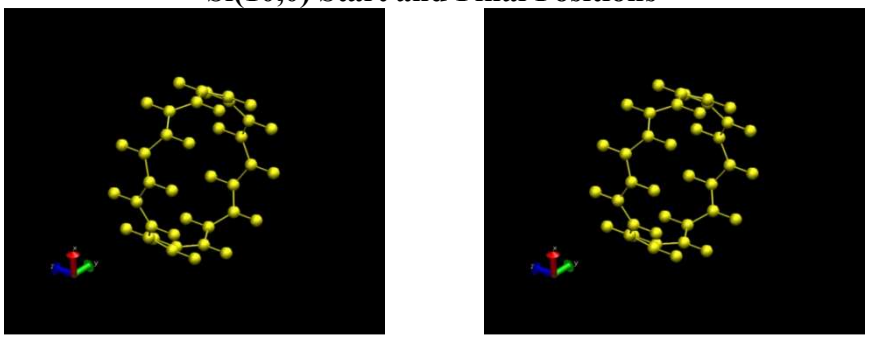

Figure 16- Si(10,0) start and final positions. Final temperature was 0.0609 K and the energy per atom was -107.15532533 eV.

C(8,0) with Si(10,0) Start and Final Positions

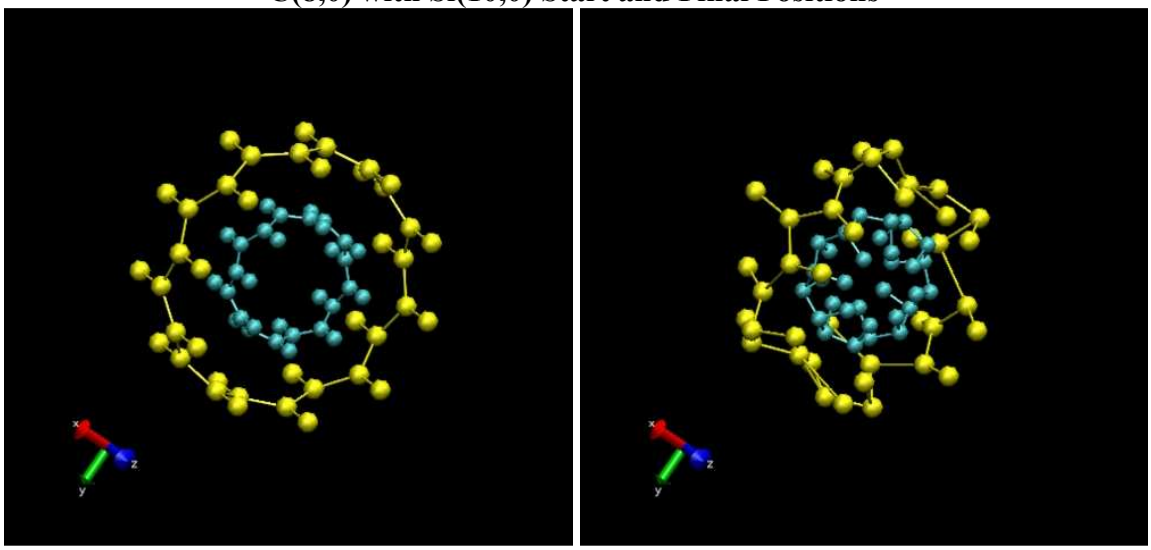

Figure 17- C(8,0) with Si(10,0) start and final positions. Final temperature was 100.3571 K and the energy per atom was -129.53142863 eV. The ending temperature was rather high for this run possibly due to the unstable nature of the tube configuration.

The final configuration I studied was 3xC(8,0) with 2xSi(10,0) and the pictures of start and final positions are shown in the figures below.

3xC(8,0) and 2xSi(10,0) Separate Final Positions

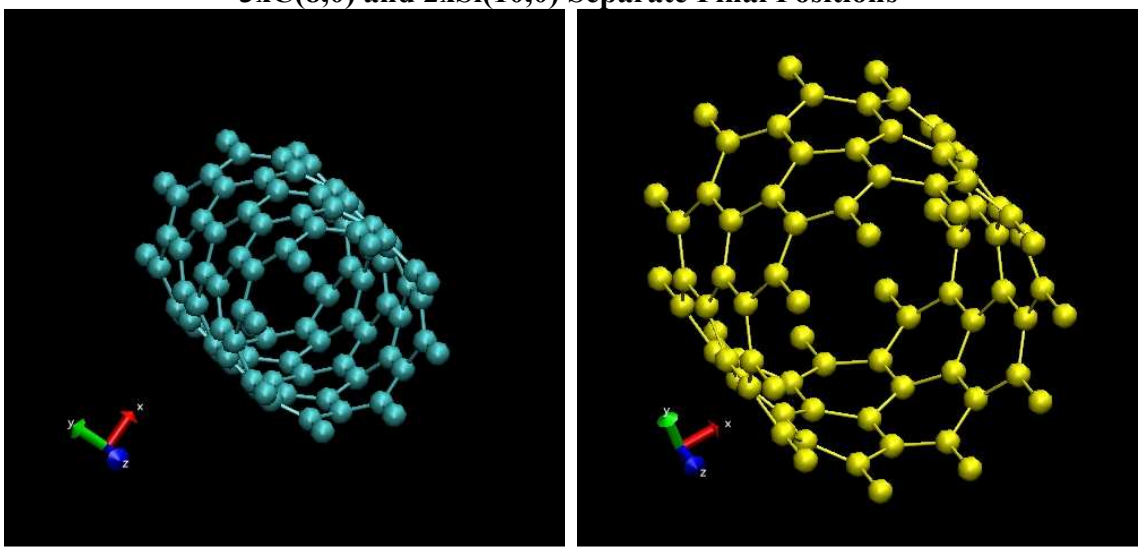

Figure 18- 3xC(8,0) (blue) and 2xSi(10,0) (yellow) separate final positions. . For carbon the final temperature was 0.0154 Kand the energy per atom was -157.67677105 eV. For silicon the final temperature was 0.0674 K and the energy per atom was -107.17493574 eV.

3xC(8,0) and 2xSi(10,0) Together Final Position

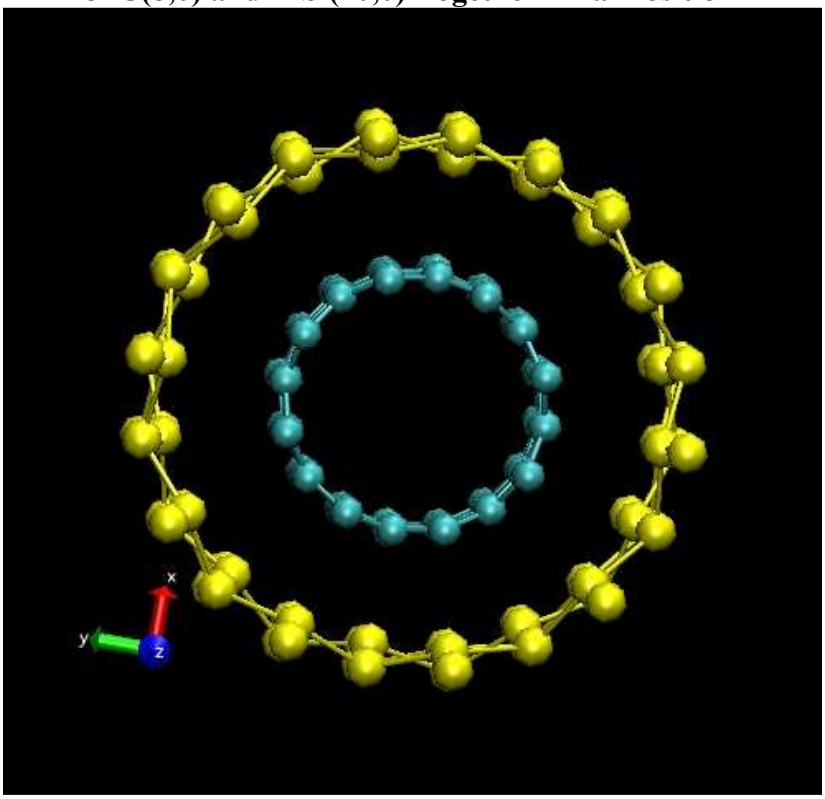

Figure 19- 3xC(8,0) with 2xSi(10,0) together final position. Final temperature was 0.2204 K and the energy per atom was -134.72527629 eV. The tubes showed very little distortion at all.

In all five of these combinations a few things remained relatively constant. The total energy of the tubes when separated is slightly more than the total energy for the combined nanotubes indicating they are more stable when combined. The other similarity they all had was that the tubes seemed to distort less when together than when they were apart. These simulations demonstrated the stability of a hexagonally bonded SiNT. Silicon prefers tetrahedral bonding so these structures would be difficult to grow but a method were introduced this simulation suggests the structures would be metastable in the planar bonds.

3.2 Stability of Separated Hexagonal SiNTs on CNTs

I used the same general format as the previous section but I wanted to test how the nanotubes would behave if I deleted certain Si atoms from the SiNT around the CNT. I did two different variations on this. The split refers to deleting atoms along the axis of the nanotube so the SiNT only partially wraps around the CNT and I did this with C(6,0) and Si(6,0). In that particular run I deleted 4 atoms forming a split along the axis of the CNT. Then I used the same approach in forming rings of SiNT around the CNT. I deleted atoms radially around the nanotube creating two separated rings that wrapped around the CNT. I did this with 3xC(8,0) and Si(10,0) with 20 atoms of Si deleted.

First I used C(6,0) with Si(6,0) together and I deleted 4 silicon atoms along the axis of the tube and then just relaxed it to test its stability. The starting and ending positions are shown in the figures.

C(6,0) with Si(6,0) Split Start and Final Positions

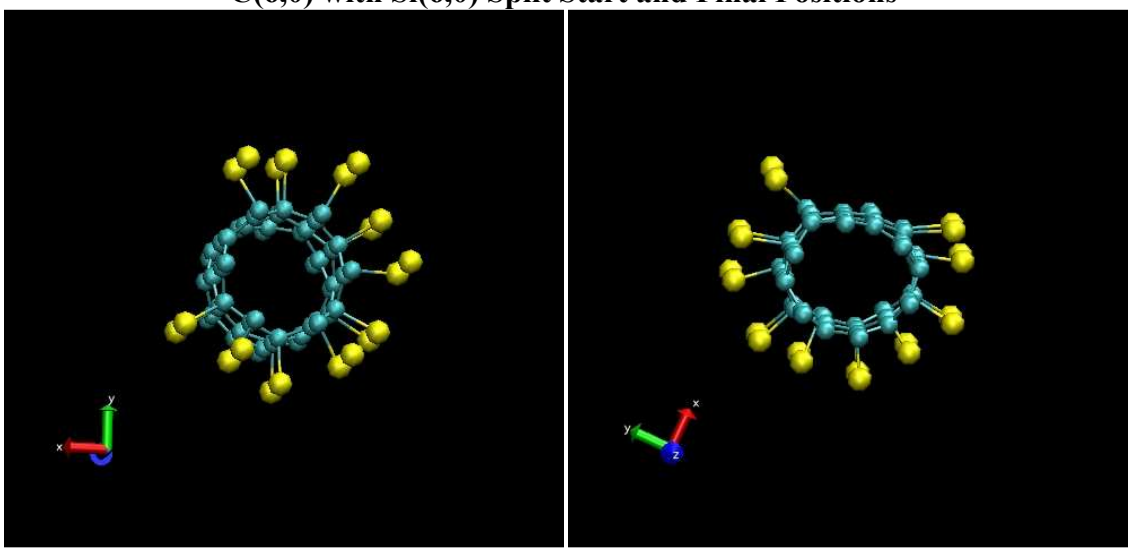

Figure 20- C(6,0) with Si(6,0) split start and final positions. The final temperature was 0.0057 K and the energy per atom was -142.72506145.

The tubes remained relatively stable while relaxing. The only visible movement is that the silicon atoms seem to bend away from the split in the SiNT. It would be interesting to further investigate that effect. It is also interesting that the silicon atoms seem to be more bonded to the CNT than with themselves.

The next study was the same principle as the split nanotubes but we deleted atoms radially instead of along the axis of the tube therefore creating a CNT surrounded by two rings of SiNT. The first rings job was done by using C(6,0) with Si(6,0) again and deleting 12 molecules. The starting and ending positions are shown below in the figures.

C(6,0) with Si(6,0) Rings Starting and Final Positions

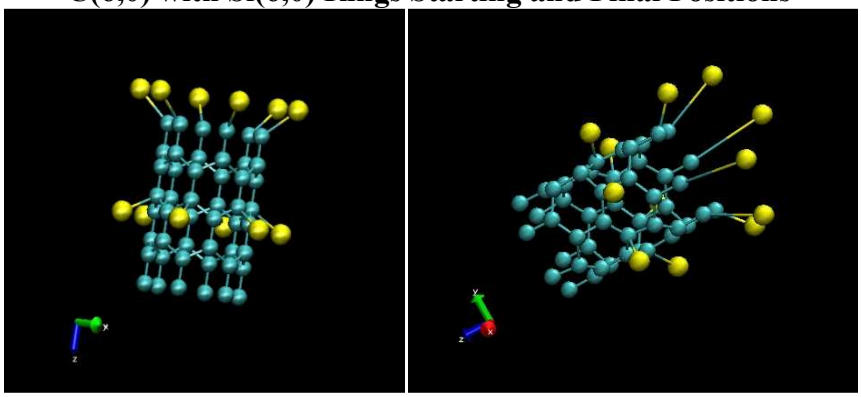

Figure 21-C(6,0) with Si(6,0) rings starting and ending positions. The final temperature was 0.2082 K and the energy per atom was -147.47249220 eV.

This run did not turn out as expected due to the small number of silicon atoms involved. The SiNT did not keep its shape at all and when it was relaxed the whole thing fell apart and disassociated. In the next rings simulation I used 3xC(8,0) with Si(10,0) with 20 radial silicon atoms deleted to form rings. This gave more of a tube shape to the SiNT even after deleting the atoms.

3xC(8,0) with Si(10,0) Rings Starting and Ending Positions

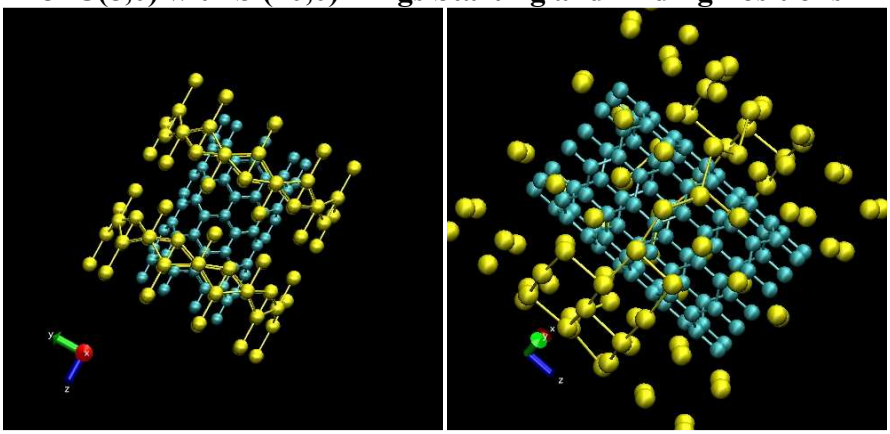

Figure 22-3xC(8,0) with Si(10,0) rings starting and ending positions. The final Temperature was approx. 200K.

The final study was cut a little bit short simply due to the amount of time it took to run the jobs on the supercomputer because of the high number of atoms. It was not relaxed to a sufficiently low temperature but the trend is definitely observable. The gap between the two rings closes completely and it forms a single SiNT around the CNT inside.

These simulations again suggest the stability of the SiNT in its hexagonally bonded form to make planar sheets analogous to those of the carbon bonds in CNTs. The silicon did not tend to bunch up and form clusters on the surface of the CNTs rather it closed the gap and made a more uniform coating around the CNT.

3.3 Energy Barriers on a Graphene Sheet

Initially this study was intended to simulate the behavior of silicon with carbon nanotubes. It was decided to first focus on and understand the simpler model of a graphene sheet. This is a natural step since a carbon nanotube is simply a graphene sheet rolled into a tube.

The simpler form of a CNT is a sheet of graphene and the diffusion of atoms on a graphene surface is analogous to the surface of a CNT. I started by generating a sheet of graphene using the lattice vectors shown in Figure 7 below. I then relaxed a silicon atom on various H sites on the graphene to use as my starting and ending positions. The numbering of the sites is shown in Figure 8 below. I then gave fireball the starting and ending positions and recorded the energy barriers that were crossed for each corresponding site on the graphene. I also performed exactly the same thing exchanging the Si atom with another C atom.

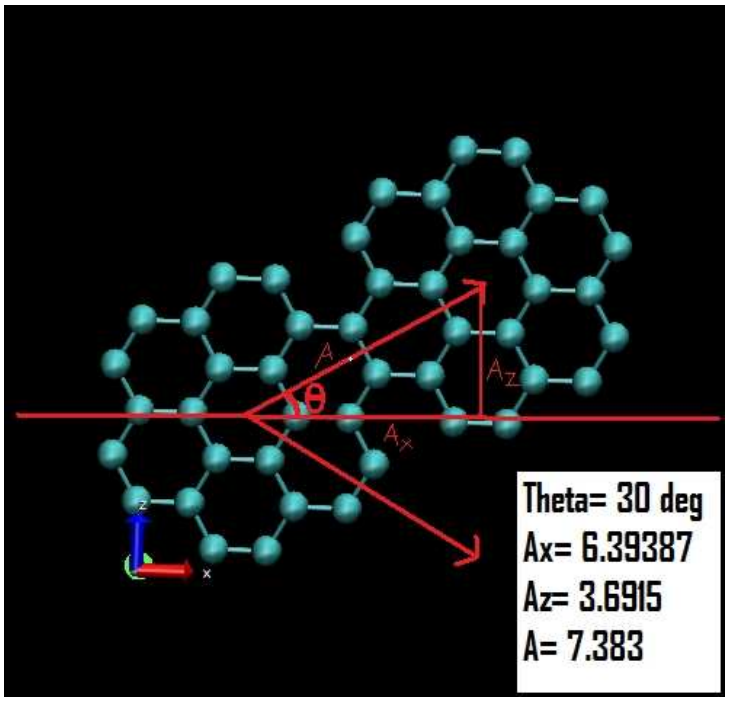

Figure 23- Lattice vectors for graphene sheet.

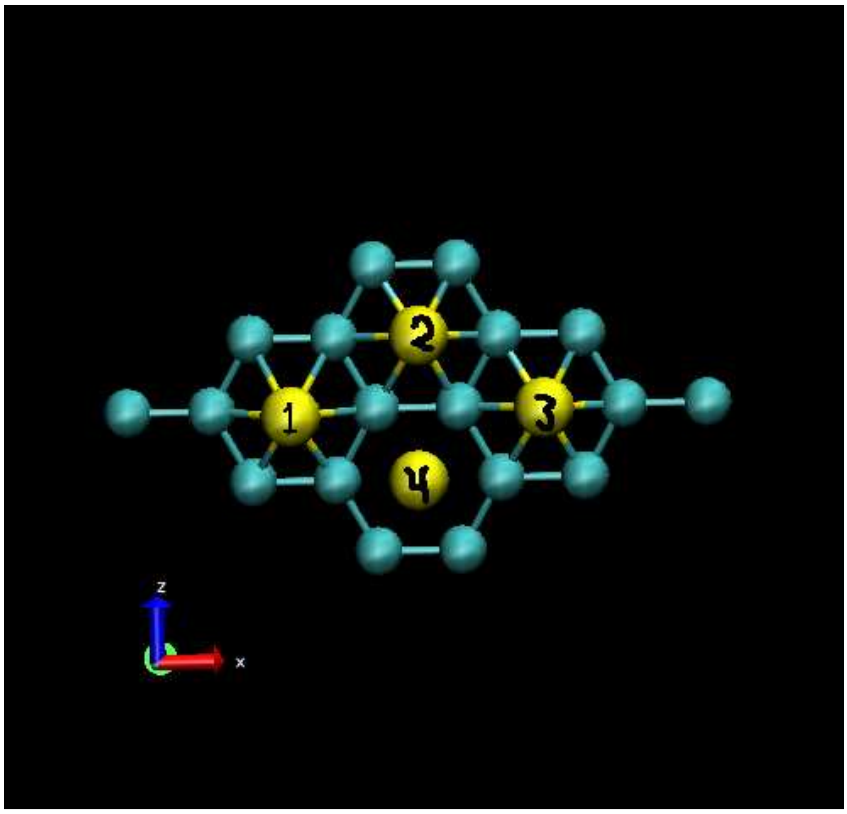

Figure 24- Starting and ending positions for the energy barrier jobs.

In order to understand which site transitions are being studied I made a reference picture of all the sites I used that are numbered as shown below in the figure.

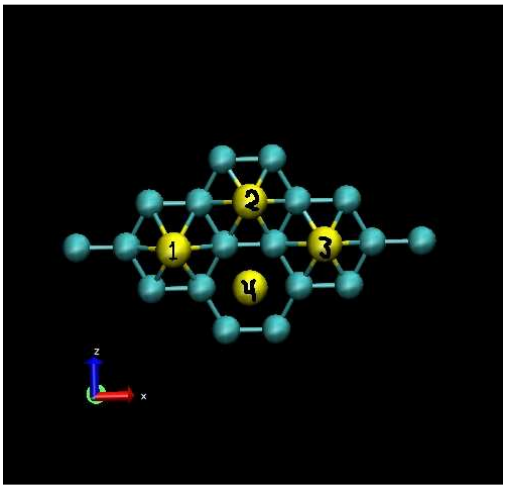

Figure 25- Numbered sites for energy barriers on graphene.

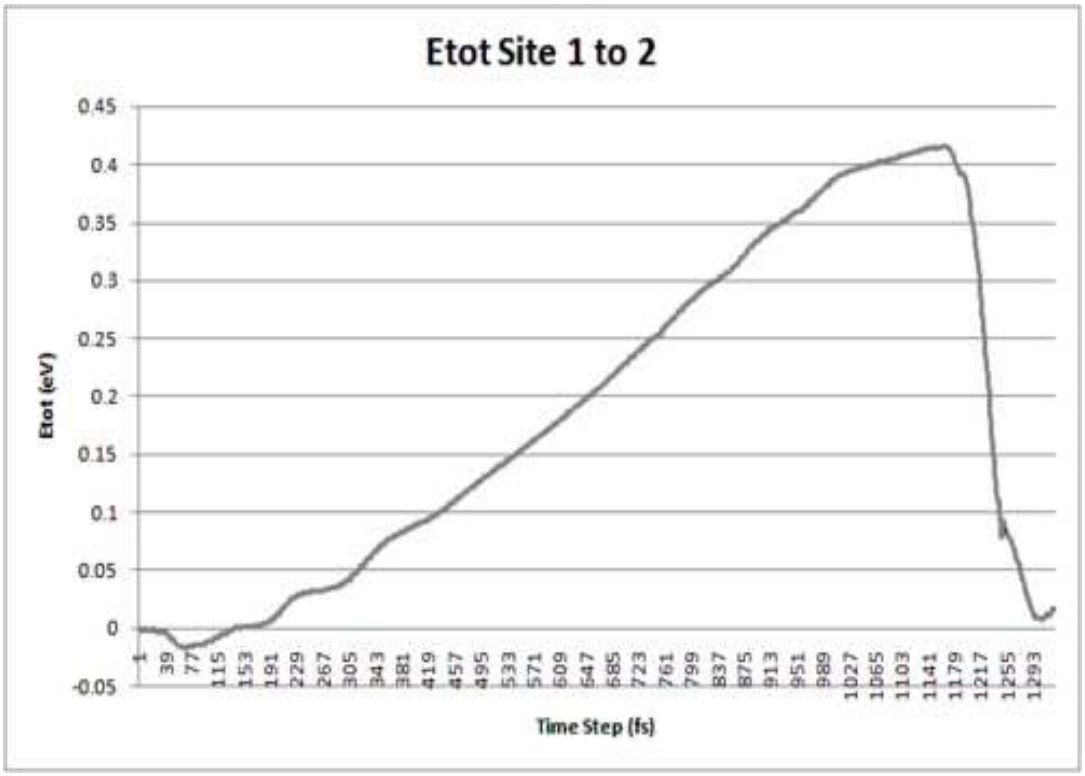

Figure 26- Total Barrier Energy Plot for Site 1 to Site 2.

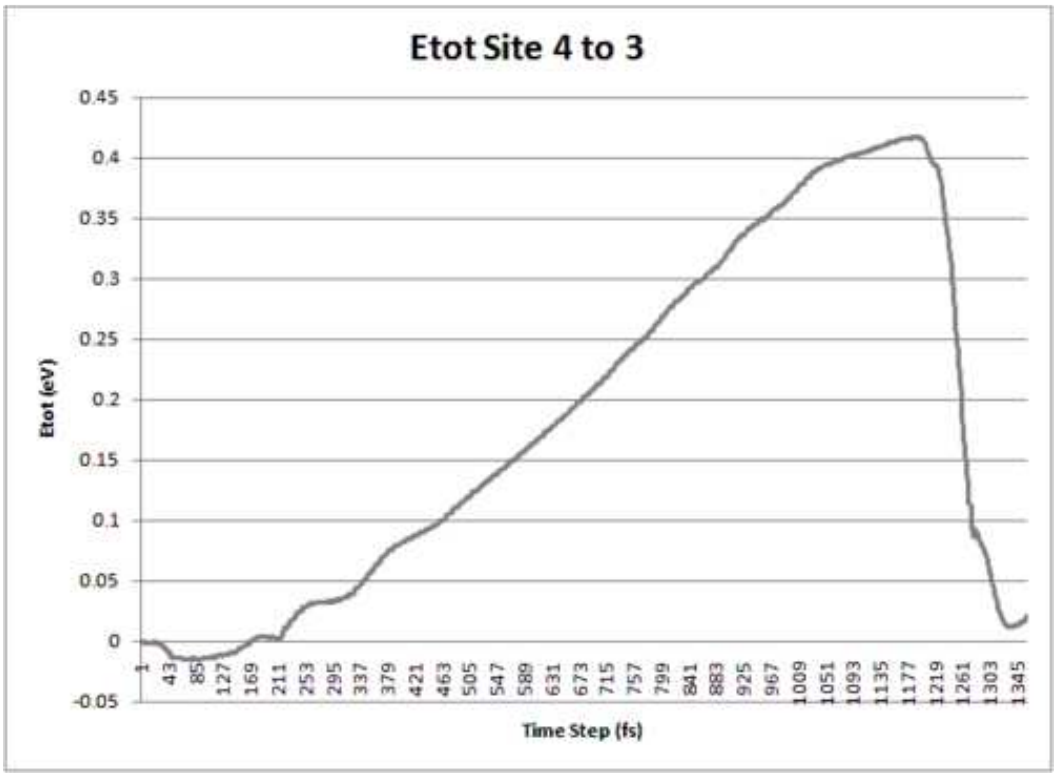

Figure 97- Total Barrier Energy Plot for Site 4 to Site 3.

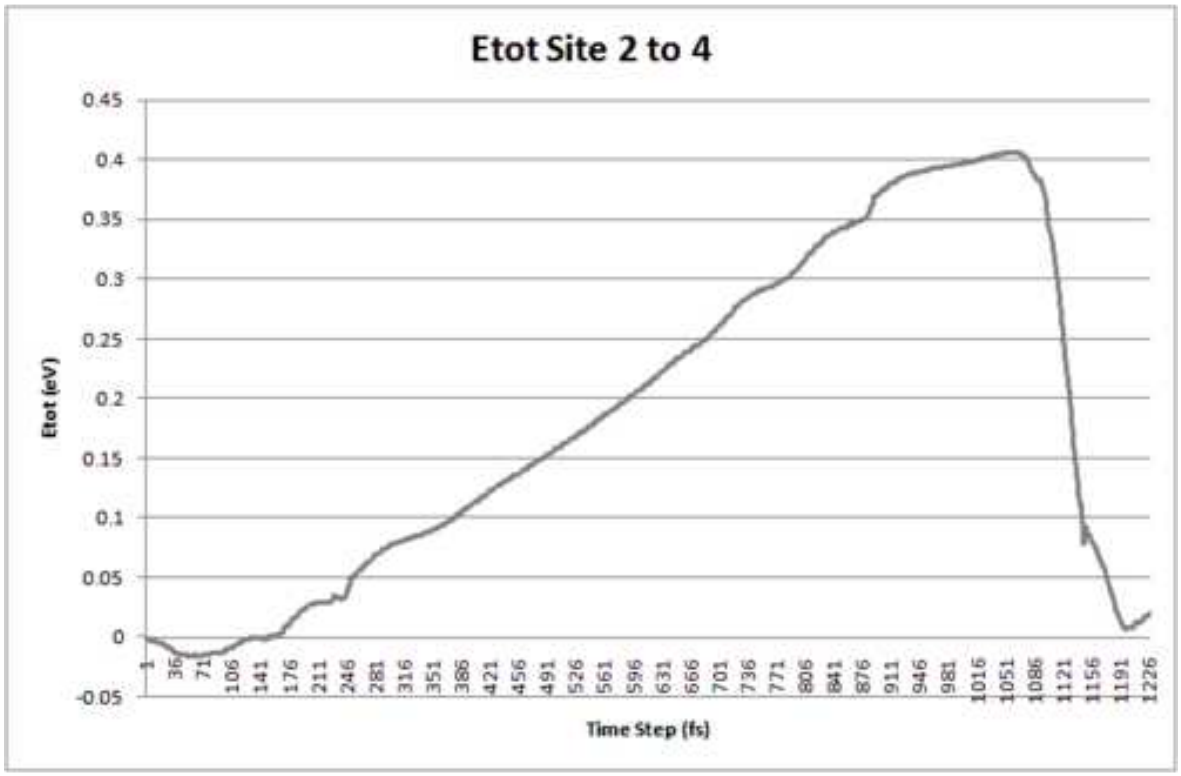

Figure 28- Total Barrier Energy Plot for Site 2 to Site 4.

From these plots it we conclude that the energy barrier for diffusion on graphite is very near 0.42 eV. It also takes approximately 130 fs for the Si atom to fall back into the well which is an important measurement when fitting data to an Arrhenius model of diffusion.

I then performed the exact same thing substituting the Si atom with another C atom in order to study the diffusion of carbon on the surface of a CNT. The sites are all numbered exactly the same and following are plots of the energy changes along the path of diffusion.

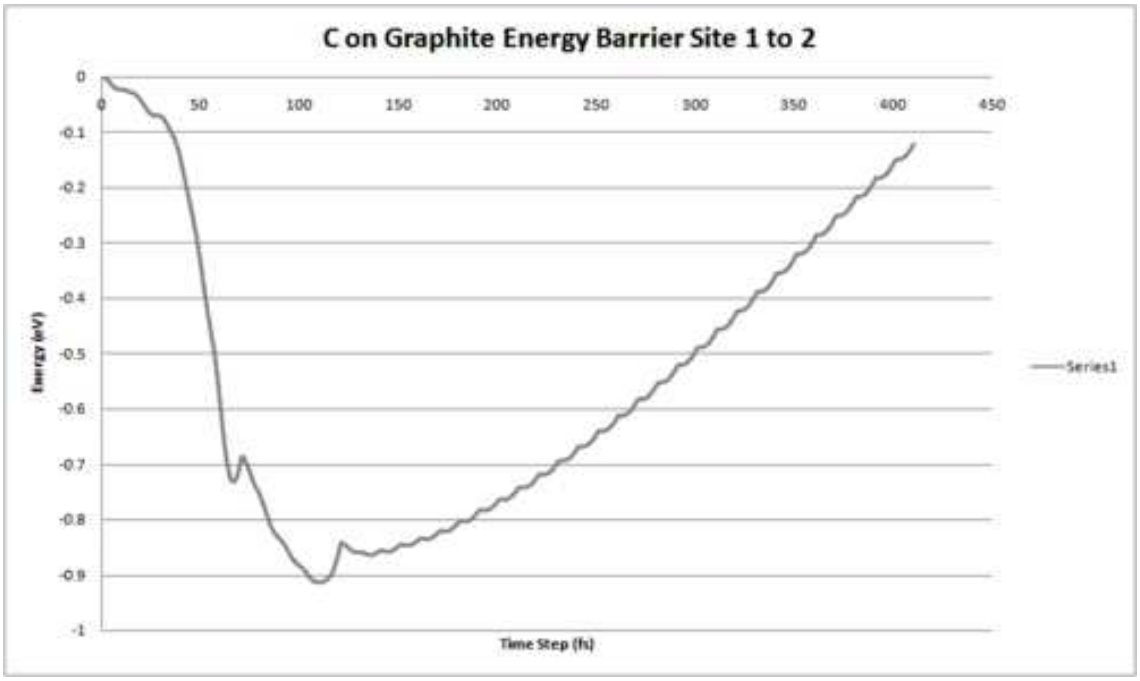

Figure 29- Energy Barrier Plot of C on Graphite from Site 1 to Site 2.

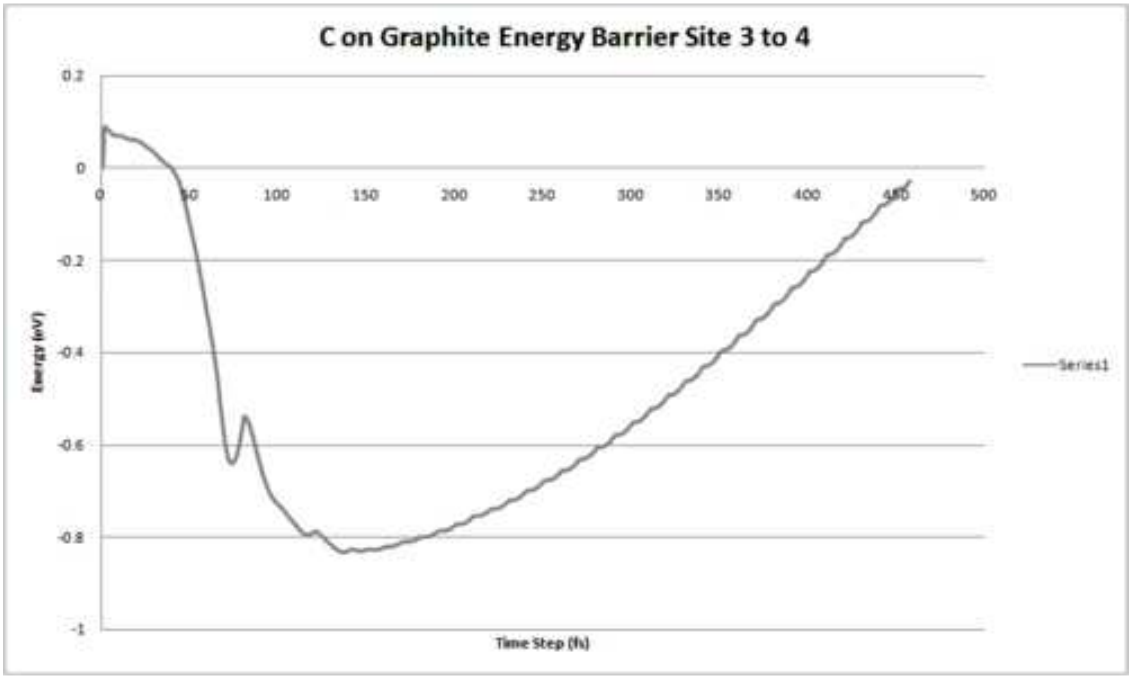

Figure 30- Energy Barrier Plot of C on Graphite from Site 3 to Site 4.

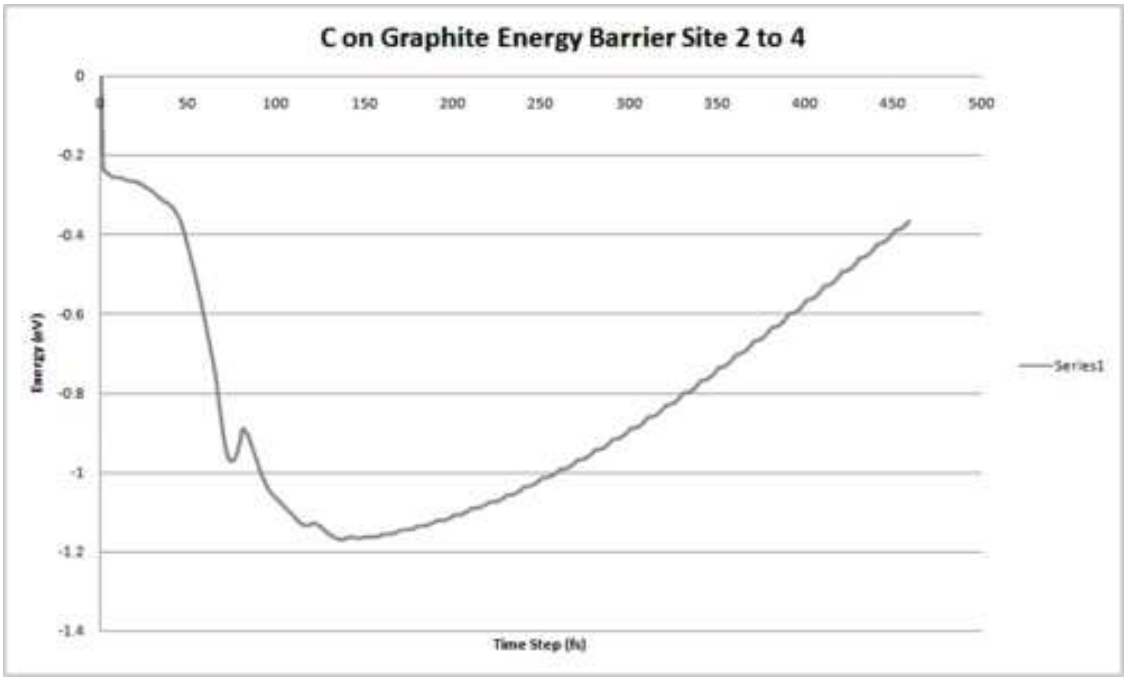

Figure 31- Energy Barrier Plot of C on Graphite from Site 2 to Site 4.

These show that carbon has different binding energies on different sites than silicon. The energy barrier for diffusion for C on a graphene sheet is approximately 1 eV.

3.4 Diffusion on a Graphene Sheet

I wanted to study diffusion of Si and C along the surface of a graphene sheet and I did so for various temperatures. In the beginning I used GULP to analyze the importance of what time step I should use. GULP was ideal for this because of the quick processing times and I was able to establish that a time step of 1 fs would be suitable for what I was trying to accomplish. I started the diffusing atom at the same position for all of the different temperatures and kept the temperature constant as the atom diffused across the surface. I used a Matlab script I wrote to count the number of "jumps" that the atom made. I defined one "jump" to be the distance between two H sites on a graphene sheet which is 2.46 angstroms. See Appendix for Matlab code.

I started a silicon atom on the same site for several different temperatures and then I used a Matlab script to count the number of "jumps" that occurred. I plotted the number of jumps versus the temperature below.

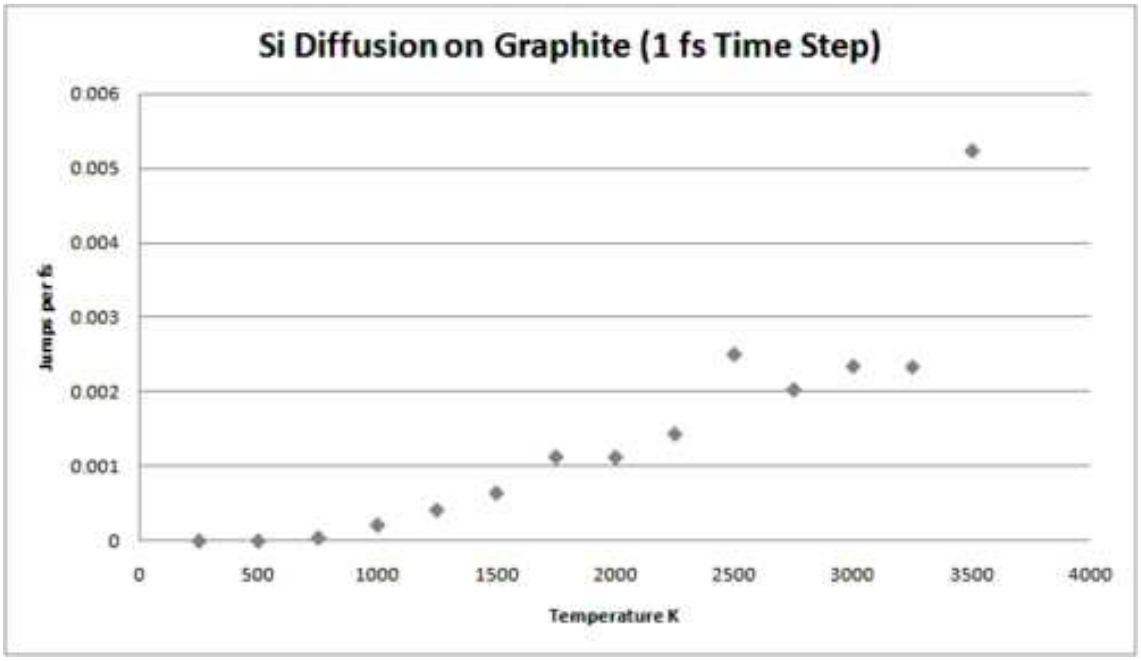

Figure 32- Si diffusion on graphite. Jumps per fs vs. temperature.

I wanted to compare the results I got with the Arrhenius model of diffusion which is defined as the following equation for the jump frequency f.

$$f = \nu * e^{\frac{-E}{K*T}}$$

In this equation ν is the "attempt frequency". Typically it is a vibrational frequency or the frequency at which the diffusing particle approaches the energy barrier. E is equal to the energy barrier and in this case it is 0.42 eV for Si on graphene. K is Boltzmann's constant and T is the temperature. I plotted my results against the theory in 3 different formats in the following figures.

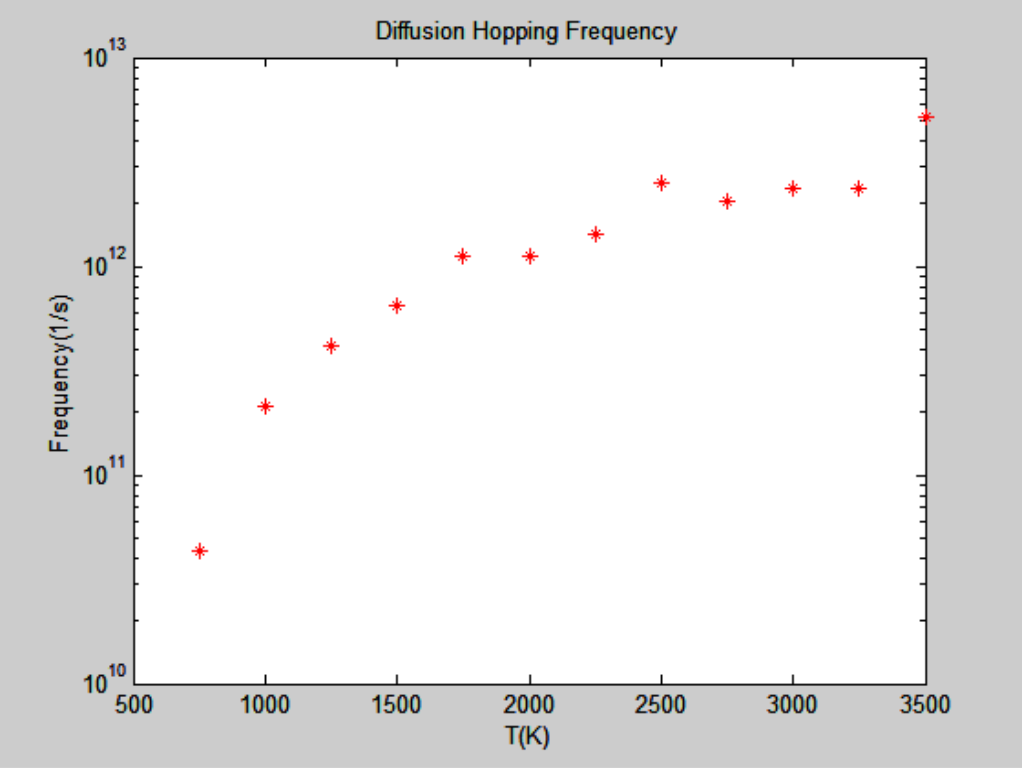

Figure 33- Frequency against Theory. Logarithmic Plot.

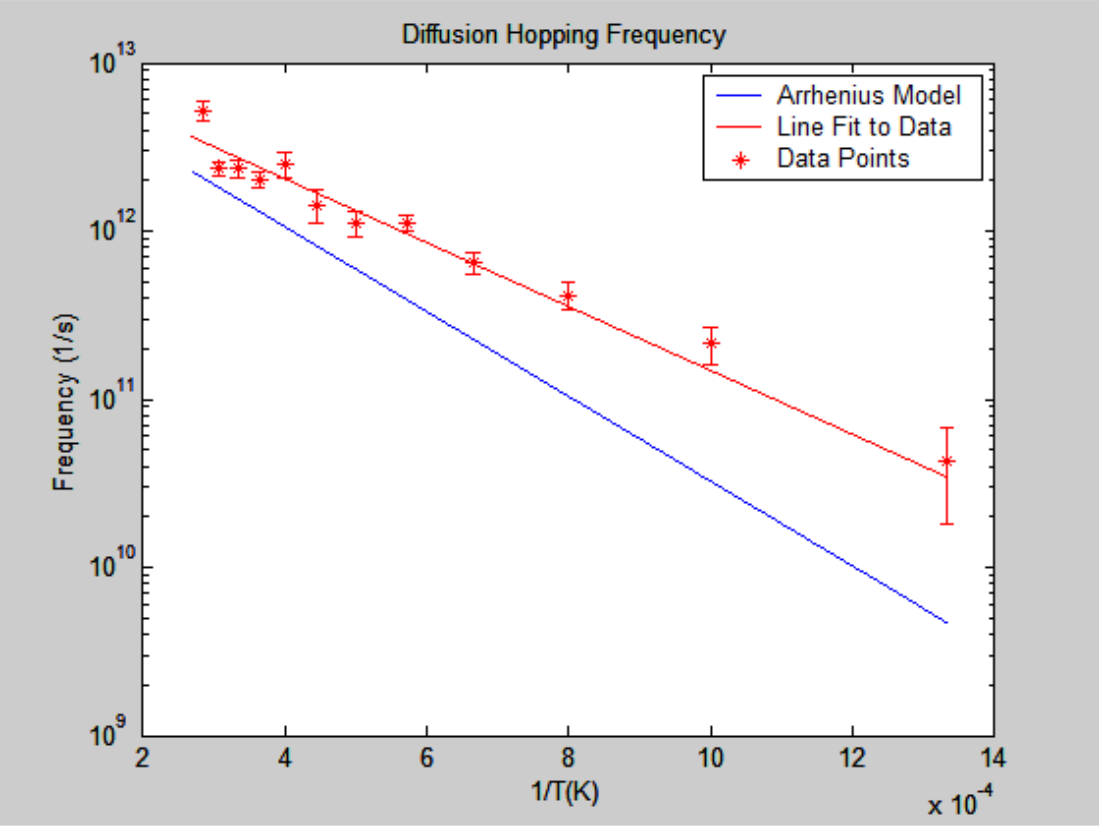

Figure 34- Frequency against Theory. Logarithmic Plot vs 1/T.

Figure 34 shows the Arrhenius model that uses the energy barrier of diffusion at zero temperature and the red line uses the energy barrier for the actual simulation. The red line that is fit to the data is definitely a different slope different energy barrier. This tells us that the energy barrier for diffusion is slightly lower at higher temperatures. The energy barrier for zero temperature was shown to be 0.42 eV where as the slope of the red line shows an energy barrier of 0.36 eV. This plot also shows that for the first few data points toward the right side of the graph the slope does appear to fit that of the Arrhenius model which we would expect because these are the lower temperatures and the model is using the zero temperature energy barrier.

Chapter 4: Conclusions

4.1 CNTs

I was able to simulate stable hexagonal SiNTs surrounding CNTs. I demonstrated that although silicon prefers tetrahedral bonding it is stable in planar hexagonal bonds. I also demonstrated that when the SiNT was broken or separated that the planar structure of the SiNT remained intact and was stable. The silicon atoms did not exhibit the tendency to form clusters on the surface of the CNT.

4.2 Graphene

I was able to successfully calculate the energy barrier for silicon on a graphene sheet to be 0.42 eV. I also calculated the energy barrier for carbon on a graphene sheet to be 0.93 eV. I also was able to model the diffusion of silicon on a graphene sheet after the simple Arrhenius model of diffusion for temperatures ranging from 500 K to 3500 K. I showed that the energy barrier for silicon on a graphene sheet does decrease as the temperature increases.

References

[1] A.V. Krasheninnikov, K. N., P.O. Lehtinen, A.S. Foster, A. Ayuela and R.M. Nieminen (2004). "Adsorption and migration of carbon adatoms on carbon nanotubes: Density-functional ab initio and tight-binding studies." Physical Review B 69.

[2] A.V. Krasheninnikov, P. O. L., A.S. Foster and R.M. Nieminen (2005). "Bending the rules: Contrasting vacancy energetics and migration in graphite and carbon nanotubes." Chemical Physics Letters 418: 132-136.

[3] Cao, B.-x. L. a. P.-l. (2004). "Silicon nanorings and nanotubes: a full-potential linear-muffin-tin-orbital molecular-dynamics method study." Journal of Molecular Structure 679: 127-130.

[4] E. Durgun, S. D., S. Ciraci, and O. Gulseren (2004). "Energetics and Electronic Structures of Individual Atoms Adsorbed on Carbon Nanotubes."Journal of Physical Chemistry B 108(Part 2): 575-582.

[5] Hideto Yoshida, T. U., Jun Kikkawa, Seiji Takeda (2007). "Growth of single-walled carbon nanotubes on silicon nanowires." Solid State Communications 141: 632-634.

[6] O'Connell, M. J. (2006). Carbon Nanotubes: Properties and Applications. Boca Raton, FL, Taylor and Francis Group.

[7] P.O. Lehtinen, A. S. F., A. Ayuela, A. Krasheninnikov, K. Nordlund and R.M. Nieminen (2003). "Magnetic properties and diffusion of adatoms on a graphene sheet." Physical Review Letters 91(Part 1): 017202.

[8] Salto, Y. U. a. M. (2008). "First-Principles Study on the Graphene Adatom and its Dimer." e-Journal of Surface Science and Nanotechnology 6: 269-271.

[9] Yanjie Gan, J. K., A.V. Krasheninnikov, K. Nordlund and F. Banhart (2008). "The diffusion of carbon atoms inside carbon nanotubes." New Journal of Physics 10.

[10] Dmitrii F. Perepichka, F. R. (2006). "Silicon Nanotubes." Small Journal 2(1): 22-25.

[11] Lewis, J. P. (2007, August 10, 2007). "Fireball Manual." Retrieved March 17, 2009, from http://fireball-dft.org/pubwiki/index.php/Fireball_Manual#FIREBALL_Introduction.

[12] Gale, J. D. General Utility Lattice Program, Nanochemistry Research Institute.

[13] TubeGen 3.3 (web-interface, http://turin.nss.udel.edu/research/tubegenonline.html), J. T. Frey and D. J. Doren, University of Delaware, Newark DE, 2005.

[14] Humphrey, W., Dalke, A. and Schulten, K., ``VMD - Visual Molecular Dynamics'' *J. Molec. Graphics* **1996**, *14.1*, 33-38.

Appendix

A-1: Counter.m

```
clear all;
close all;
clc;
L = 2.46;
load c3750k.dat;
x = c3750k(:,1);
y = c3750k(:,2);
z = c3750k(:,3);
N = length(x);
c = 0;

rhome= [x(1) , y(1), z(1) ]; % first one!
for i=1:19:N;
   rcurrent = [x(i) , y(i), z(i) ];
   deltar = rcurrent - rhome;
   distance = sqrt( dot(deltar, deltar) );
   if distance >= L;
      c= c+1
      rhome= rcurrent;

   end
end
```

…second through the eighteenth

```
rhome= [x(19) , y(19), z(19) ]; % ninteenth one!
for i=19:19:N;
   rcurrent = [x(i) , y(i), z(i) ];
   deltar = rcurrent - rhome;
   distance = sqrt( dot(deltar, deltar) );
   if distance >= L;
      c= c+1
      rhome= rcurrent;

   end
end
fprintf('c = %g \n',c);
```